

SFB 649 Discussion Paper 2009-001

Implied Market Price of Weather Risk

Wolfgang Karl Härdle*
Brenda López Cabrera*

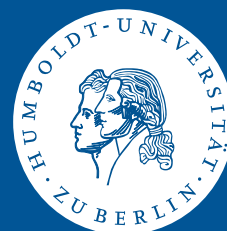


*Humboldt-Universität zu Berlin, Germany

This research was supported by the Deutsche
Forschungsgemeinschaft through the SFB 649 "Economic Risk".

<http://sfb649.wiwi.hu-berlin.de>
ISSN 1860-5664

SFB 649, Humboldt-Universität zu Berlin
Spandauer Straße 1, D-10178 Berlin



SFB 649 ECONOMIC RISK BERLIN

Implied Market Price of Weather Risk

Wolfgang Karl Härdle, Brenda López Cabrera

CASE - Center for Applied Statistics and Economics
Humboldt-Universität zu Berlin

Abstract

Weather influences our daily lives and choices and has an enormous impact on corporate revenues and earnings. Weather derivatives differ from most derivatives in that the underlying weather cannot be traded and their market is relatively illiquid. The weather derivative market is therefore incomplete. This paper implements a pricing methodology for weather derivatives that can increase the precision of measuring weather risk. We applied continuous autoregressive models (CAR) with seasonal variation to model the temperature in Berlin and with that to get explicit nature of non-arbitrage prices for temperature derivatives. We infer the implied market price from Berlin cumulative monthly temperature futures that are traded at the Chicago Mercantile Exchange (CME), which is an important parameter of the associated equivalent martingale measures used to price and hedge weather future/options in the market. We propose to study the market price of risk, not only as a piecewise constant linear function, but also as a time dependent. In any of the previous cases, we found that the market price of weather risk is different from zero and shows a seasonal structure. With the extracted information we price other exotic options, such as cooling/heating degree day temperatures and non standard contract with crazy maturities.

Keywords: Weather derivatives, weather risk, weather forecasting, seasonality, continuous autoregressive model, stochastic variance, CAT index, CDD index, HDD index, market price of risk, risk premium, CME

JEL classification: G19, G29, N26, N56, Q29, Q54

Acknowledgements: The financial support from the Deutsche Forschungsgemeinschaft via SFB 649 "Ökonomisches Risiko", Humboldt-Universität zu Berlin is gratefully acknowledged.

1 Introduction

Weather influences our daily lives and has an enormous impact on corporate revenues and earnings. The global climate changes the volatility of weather and the occurrence of extreme weather events increases. Disfavoured extreme natural events like hurricanes, long cold winter, heat, drought, freeze, etc. may cause substantial financial losses. The traditional way of protection against unpredictable weather conditions is the insurance, which covers the losses in exchange for the payment of a premium. However, recently one observes an inception of new financial instruments linked to weather conditions: CAT bonds, sidecars and weather derivatives.

In the 1990's Weather Derivatives (WD) were developed to hedge against volatility caused by weather. WD are financial contracts, which payments are based on weather-related measurements. They are formally exchanged in the Chicago Mercantile Exchange (CME), where monthly and seasonal temperature future, call and put options contracts on future prices are traded. The futures and options at CME are cash settled. WDs cover against extreme changes on temperature, rainfall, wind, snow, frost, but do not cover catastrophic events, such as hurricanes. According to the CME (2006), the WD market has increased notably from 2.2 billion USD in 2004 to 22 billion USD through September 2005.

The key factor in efficient usage of WD's is a reliable valuation procedure. However, due to their specific nature one suffers several difficulties. First, weather derivatives are different from most financial derivatives because the underlying weather cannot be traded. Second, the weather derivatives market is relatively illiquid, i.e. the weather derivatives cannot be cost-efficiently replicated with other weather derivatives.

In practice, the valuation of WD is in spirit and methodology closer to insurance pricing than to derivative pricing (arbitrage pricing) since their values equal to the expected outcome under the physical probability plus a charge depending on a risk measure (usually the standard deviation) ?.

The pricing of weather derivatives attracted the attention of many researchers. ? fitted an Ornstein-Uhlenbeck stochastic process with constant variance to temperature observations at Chicago O'Hare airport and started to investigate future prices on temperature indices. Later ? applied the Ornstein-Uhlenbeck model with a monthly variation in the variance to temperature data of Bromma airport (Stockholm). They applied their model to get prices for different temperature prices. ? modelled temperature in several US cities with a higher order autoregressive model. They observed seasonality behaviour in the autocorrelation function (ACF) of the squared residuals. However, they did not price temperature derivatives. ? studied the temperature in Casablanca, Morocco using a mean reverting model with stochastic volatility and a temperature swap was considered. ? calculates an arbitrage free price for different temperature derivatives prices by using the fractional Brownian motion model of ?, which drives the noise in an Ornstein-Uhlenbeck process.

In the temperature derivative market, ? proposed to use a marginal utility technique to price temperature derivatives based on the HDD index. ? present an optimal design of weather derivatives in an illiquid framework, arguing that the standard risk neutral point of view is not applicable to value them. ? and ? apply an extended version of Lucas' (1978) equilibrium pricing model where direct estimation of market price of weather risk is avoided. Instead, pricing is based on the stochastic processes of the weather index, an aggregated dividend and an assumption about the utility function of a representative investor. ? used the world stock index as the numeraire to price temperature derivatives. ? and (2007) propose the continuous time autoregressive model with seasonality for the temperature evolution in time and fit this model to data observed in Stockholm, Sweden. They derive future and option prices for contracts on CDD and CAT indices. They also discuss hedging strategies for the options and volatility term structure. For pricing a New York WD, ? carried out an empirical study for the New York over the counter (OTC) future prices and other weather contracts to extract the risk neutral distribution and the market price of weather risk. ? extended the long term temperature model proposed by ? by taking into account ARCH/GARCH effects to reflect the clustering of volatility temperature. They examine the effects of mean, variance and market price of risk on HDD/CDD option prices and demonstrate that their effect are similar to those on the prices of traditional options.

In this paper, we apply continuous autoregressive models (CAR) with seasonal variation to model the temperature in Berlin, as ? did for Stockholm Temperature data in order to get the explicit nature of non-arbitrage prices for temperature derivatives. Contrast to this work we find that Berlin Temperature is more normal in the sense that the driving stochastics are closer to a Wiener Process than their analysis for Stockholm. The estimate of the market price of weather risk (MPR) is interesting by its own and has not been studied earlier. The MPR adjusts the underlying process so that the level the risk aversion is not needed for valuation. The majority of papers so far have solved it assuming zero MPR, but this assumption underestimates WD prices. By using the theoretical explicit prices we imply the market price of temperature risk for Berlin futures. We find that the market price of risk is different from zero. We show the seasonal structure when the MPR is assumed to be piecewise constant linear function of time dependent. Not only, the importance of the MPR estimate is for pricing derivatives (future/options) but also for hedging and for pricing new non standard contracts with "nonstandard maturities" and other OTC contracts. By using the implied MPR from Berlin Cumulative Average Temperature (CAT) futures, we price new derivatives, e.g. Cold Degree Days (CDD) and Heating Degree Days (HDD) for Berlin. A clear seasonal variation in the regression residuals of the temperature is observed and the volatility term structure of CAT temperature futures presents a modified Samuelson effect.

Our paper is structured as follows. In the next section -the econometric part- is devoted to explain the dynamics of Berlin temperature data by using by a continuous autoregressive model (CAR). In section 3, we discuss fundamentals of temperature derivatives (future and options), their indices and also we describe the monthly temperature futures traded at CME, the biggest market offering this kind of product. In section 4, the financial mathematics part of the paper is explained when we connect the weather with the pricing dynamics. We implied the market price of risk for Berlin monthly temperature futures which are traded at the Chicago Mercantile Exchange (CME). We study the market price of risk, not only as a piecewise constant linear function, but also as time dependent for different contract types. In any of the previous cases, we found that the market price of weather risk is different from zero and shows a seasonal structure. With the extracted information we price other exotic options, such as cooling/heating degree day temperatures and non standard contract with crazy maturities. Section 5 concludes. All computations in this paper were made in Matlab version 7.6.

2 Berlin temperature dynamics

In this section, we study the weather dynamics for Berlin daily temperature data. The temperature data was obtained from the Deutscher Wetterdienst. It considers 22063 recordings of daily average temperatures from 19500101-20080527 at the Tempelhof Airport Station. Figure 1 we display for a better exposition a structure of 8.5 years. We observe low temperatures in the winter and high temperatures in the summer.

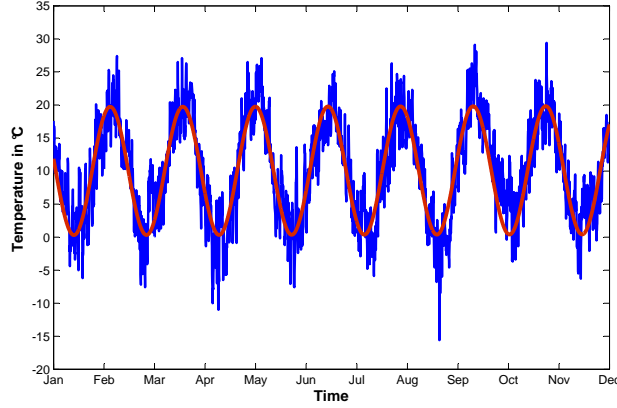


Figure 1: Seasonality effect (red line) and daily average temperature from Berlin 2000101-20080527, weather station: Tempelhof Airport Station.

We first check the presence of a linear trend and investigate the seasonal pattern of the data. A linear trend was not detectable,

$$\Lambda_t = a_0 + a_1 t + a_2 \cos \left\{ \frac{2\pi(t - a_3)}{365} \right\} \quad (1)$$

where $\hat{a}_0 = 91.52$, $\hat{a}_1 = 0.00$, $\hat{a}_2 = 97.96$, $\hat{a}_3 = -165.1$ with 95% confidence bounds and R^2 equal to 0.7672.

After removing the seasonality (equation 1) from the daily average temperatures,

$$X_t = T_t - \Lambda_t \quad (2)$$

we check whether X_t is a stationary process $I(0)$. In order to do that, we apply the Augmented Dickey-Fuller test (ADF):

$$(1 - L)X = c_1 + \mu t + \tau LX + \alpha_1(1 - L)LX + \dots \alpha_p(1 - L)L^p X + \varepsilon_t$$

where the test statistic for a unit root in a time series $\tau = -35.001$, with 1% critical value equal to -2.56. We reject the null hypothesis H_0 ($\tau = 0$) and hence Y_i is a stationary process $I(0)$. This result can also be verified by using the KPSS Test:

$$X_t = c + \mu t + k \sum_{i=1}^t \xi_i + \varepsilon_t$$

We accept $H_0 : k = 0$ at 10% significance level that the process is stationary. The test statistic for the constant is equal to 0.653 and for the trend equal to 0.139.

The Partial Autocorrelation Function (PACF) of Equation 2 is plotted in Figure 2. The PACF suggests that the AR(3) model suggested by ? also holds for Berlin Temperature data. The fitted autoregressive process is equal to: $X_{t+3} = 0.91X_{t+2} - 0.20X_{t+1} + 0.08X_t + \sigma_t \varepsilon_t$.

The residuals and squared residuals of the Berlin Temperature data, after trend and seasonal component were removed, are plotted in Figure 3. According to the modified Li-McLeod Portmanteau test, we reject at 0% significance level the null hypothesis H_0 that the residuals are uncorrelated. The ACF of the residuals of AR(3), upper panel in Figure 4, is close to zero and according to Box-Ljung statistic the first few lags are insignificant.

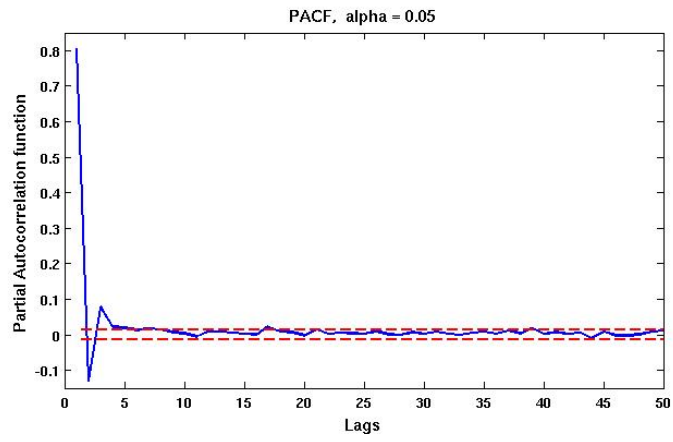


Figure 2: Partial autocorrelation function (PACF) for X_t 19480101-20080527

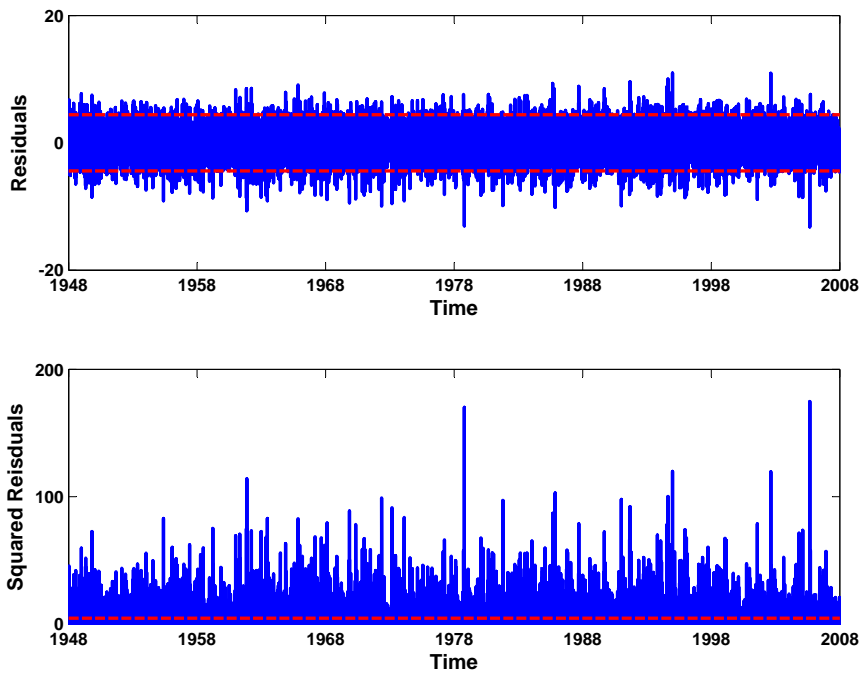


Figure 3: Residuals $\hat{\varepsilon}_t$ (up) and squared residuals $\hat{\varepsilon}_t^2$ (down) of the AR(3) during 19480101-20080527

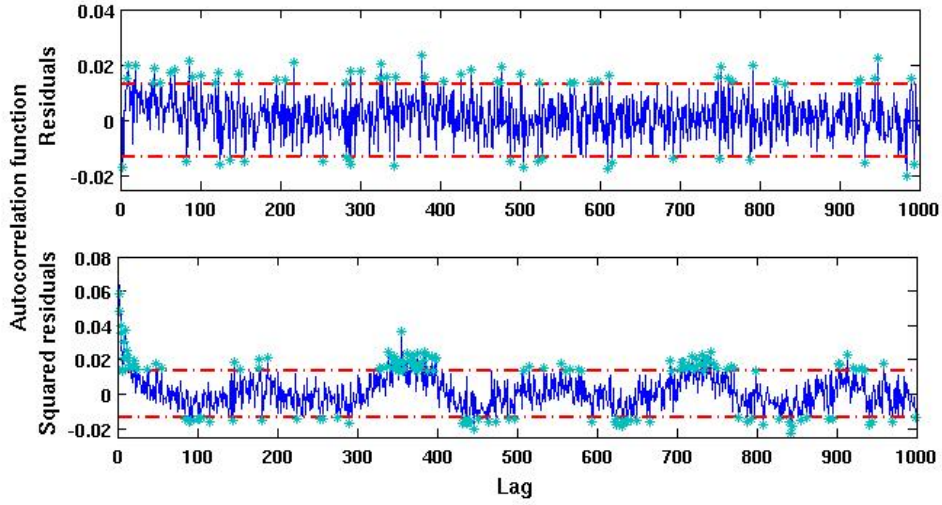


Figure 4: ACF for residuals $\hat{\epsilon}_t$ (up) and squared residuals $\hat{\epsilon}_t^2$ (down) of the AR(3) during 19480101-20080527

But, the ACF for the squared residuals in the lower panel Figure 4 shows a high seasonality pattern. We calibrate this seasonal dependence of variance of residuals of the AR(3) for 57 years with a truncated Fourier function

$$\sigma_t^2 = c_1 + \sum_{i=1}^4 \left\{ c_{2i} \cos\left(\frac{2i\pi t}{365}\right) + c_{2i+1} \sin\left(\frac{2i\pi t}{365}\right) \right\} \quad (3)$$

Alternatively one could have smoothed the data with a kernel regression estimator. Asymptotically they can be approximated by Fourier series estimators though. Figure 5 shows the daily empirical variance (the average of squared residuals for each day of the year) and the fitted squared volatility function for the residuals. Here we obtain the ? effect for Stockholm temperature data, high variance in winter - earlier summer and low variance in spring - late summer. Figure 6 shows the Berlin temperature residuals $\hat{\epsilon}_t$ and squared residuals $\hat{\epsilon}_t^2$ after correcting for seasonal volatility σ_t . Figure 6 shows the time series of residuals and squared residuals after

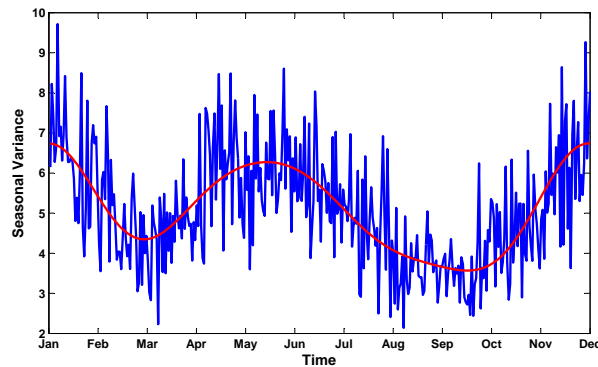


Figure 5: Seasonal variance: daily empirical variance (blue line), fitted squared volatility function (red line) at 10% significance level. $\hat{c}_1 = 5.09$, $\hat{c}_2 = 0.64$, $\hat{c}_3 = 0.74$, $\hat{c}_4 = 0.95$, $\hat{c}_5 = -0.45$, $\hat{c}_6 = 0.44$, $\hat{c}_7 = 0.05$, $\hat{c}_8 = 0.81$, $\hat{c}_9 = 0.81$

dividing out the seasonal volatility from the regression residuals, we observed closed to normal residuals. We observed that the ACF plot of the residuals remain unchanged and now the ACF plot for squared residuals presents a non-seasonal pattern, Figure 7.

The Ljung-Box's test statistic (Qstat) is used to to check the significance level of the lags of the ACF of residuals

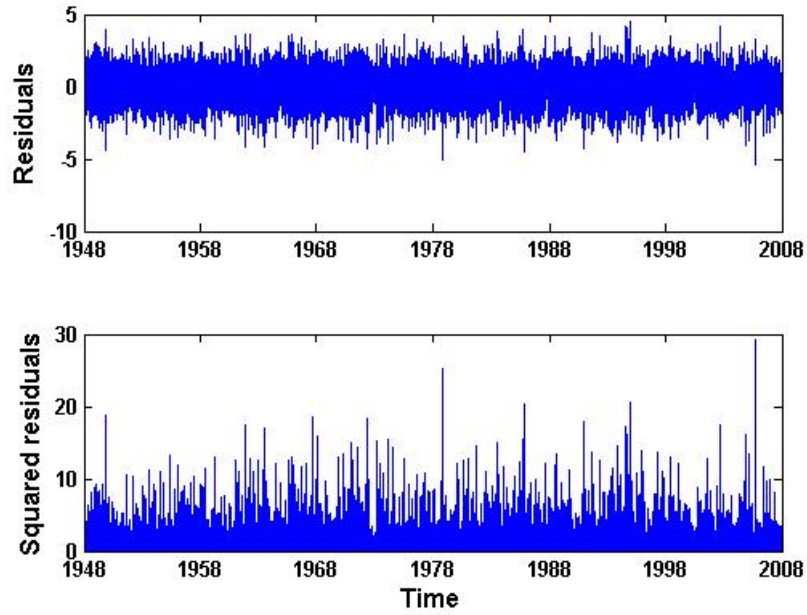


Figure 6: Berlin temperature residuals $\hat{\varepsilon}_t$ (up) and squared residuals $\hat{\varepsilon}_t^2$ (down) after correcting for seasonal volatility

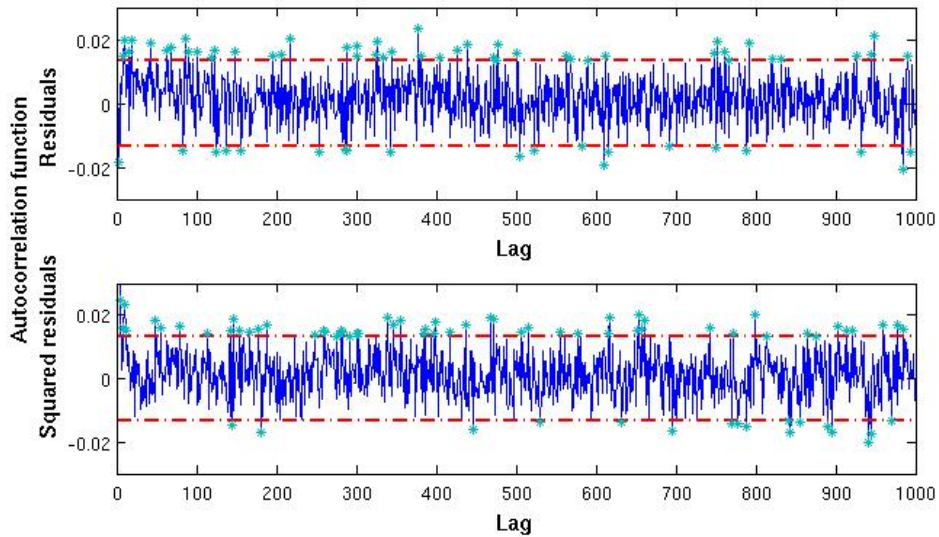


Figure 7: ACF for Berlin temperature residuals $\hat{\varepsilon}_t$ (up) and squared residuals $\hat{\varepsilon}_t^2$ (down) after correcting for seasonal volatility

Lag	$Qstat_{res}$	$QSIG_{res}$	$Qstat_{res1}$	$QSIG_{res1}$
1	0.03	0.85	0.67	0.41
2	0.05	0.97	0.74	0.69
3	3.16	0.36	4.88	0.18
4	4.70	0.32	6.26	0.18
5	4.76	0.44	6.67	0.24
6	5.40	0.49	7.17	0.30
7	6.54	0.47	7.51	0.37
8	10.30	0.24	10.34	0.24
9	14.44	0.10	14.65	0.10
10	21.58	0.01	21.95	0.10

Table 1: Q-test (Qstat) using Ljung-Box's and the corresponding significance levels (QSIG) for residuals with (res) and without seasonality in the variance (res1)

with and without seasonal volatility. Table 1 presents the statistics and the corresponding significance levels of the lags.

we plot the Kernel smoothing density estimate against a Normal Kernel evaluated at 100 equally spaced points for Berlin temperature residuals in the left side of Figure 8 to verify if residuals become normal distributed. The obtained residuals have a skewness equal to -0.08, a kurtosis equal to 3.56 and Jarques Bera statistics equal to 318.96. The acceptance of the null hypothesis H_0 of normality is at 1% significance level. right side of Figure 8 shows the log of the estimated distribution function.

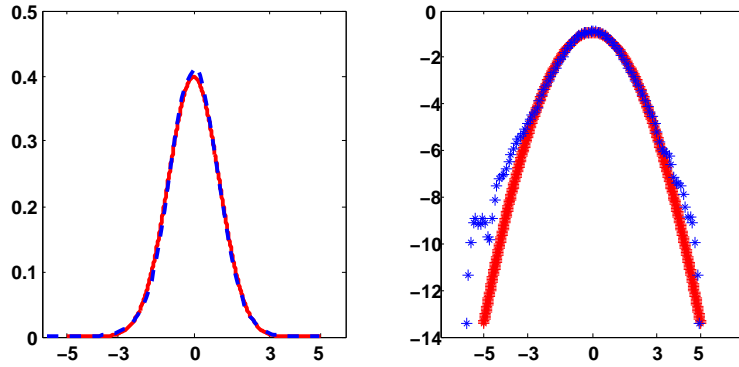


Figure 8: Left side: the Kernel smoothing density estimate (blue line) vs Normal Kernel (red line) for Berlin temperature residuals, right side: log of the estimated distribution function

Draw up on Markov property, future states are independent of the past states, the q 'th coordinate of vector \mathbf{X} with $q = 1, \dots, p$, X_q from the temperature time series:

$$T_t = \Lambda_t + X_{1t} \quad (4)$$

can as a discretization of a continuous-time process AR(p) ($CAR(p)$). As described in the next section, this stochastic model will allow CAR(p) futures/options pricing.

Define a $p \times p$ -matrix:

$$A = \begin{pmatrix} 0 & 1 & 0 & \dots & 0 & 0 \\ 0 & 0 & 1 & \dots & 0 & 0 \\ \vdots & & & \ddots & & \vdots \\ 0 & \dots & \dots & & 0 & 0 & 1 \\ -\alpha_p & -\alpha_{p-1} & \dots & & 0 & -\alpha_1 \end{pmatrix} \quad (5)$$

in the vectorial Ornstein-Uhlenbleck process $\mathbf{X}_t \in \mathbb{R}^p$ for $p \geq 1$ as:

$$d\mathbf{X}_t = A\mathbf{X}_t dt + \mathbf{e}_{pt}\sigma_t dB_t \quad (6)$$

where \mathbf{e}_k denotes the k 'th unit vector in \mathbb{R}^p for $k = 1, \dots, p$, $\sigma_t > 0$ states the temperature volatility, B_t is a Wiener Process and α_k are positive constants.

By applying the multidimensional *Itô Formula*, the process 6 with $\mathbf{X}_t = \mathbf{x} \in \mathbb{R}^p$ has the explicit form:

$$\mathbf{X}_s = \exp \{A(s-t)\} \mathbf{x} + \int_t^s \exp \{A(s-u)\} \mathbf{e}_p \sigma_u dB_u \quad (7)$$

for $s \geq t \geq 0$ and stationarity holds when the eigenvalues of A have negative real part or the variance matrix

$$\int_0^t \sigma_{t-s}^2 \exp \{A(s)\} \mathbf{e}_p \mathbf{e}_p^\top \exp \{A^\top(s)\} ds \quad (8)$$

converges as $t \rightarrow \infty$.

Iteratively into the discrete-time dynamics, one obtains the discrete version of the $CAR(p)$ process 6. For example, when $p = 1, 2, 3$ and using $\varepsilon_t = B_{t+1} - B_t$, we repeat the exercise:

for $p = 1$, we get that $\mathbf{X}_t = X_{1t}$ and $dX_{1t} = -\alpha_1 X_{1t} dt + \sigma_t dB_t$.

for $p = 2$, we have:

$$X_{1(t+2)} \approx (2 - \alpha_1) X_{1(t+1)} + (\alpha_1 - \alpha_2 - 1) X_{1(t)} + \sigma_t (B_{t-1} - B_t)$$

for $p = 3$, iterations yield:

$$\begin{aligned} X_{1(t+1)} - X_{1(t)} &= X_{1(t)} dt + \sigma_t \varepsilon_t \\ X_{2(t+1)} - X_{2(t)} &= X_{3(t)} dt + \sigma_t \varepsilon_t \\ X_{3(t+1)} - X_{3(t)} &= -\alpha_3 X_{1(t)} dt - \alpha_2 X_{2(t)} dt - \alpha_1 X_{3(t)} dt + \sigma_t \varepsilon_t \\ X_{1(t+2)} - X_{1(t+1)} &= X_{1(t+1)} dt + \sigma_{t+1} \varepsilon_{t+1} \\ X_{2(t+2)} - X_{2(t+1)} &= X_{3(t+1)} dt + \sigma_{t+1} \varepsilon_{t+1} \\ X_{3(t+2)} - X_{3(t+1)} &= -\alpha_3 X_{1(t+1)} dt - \alpha_2 X_{2(t+1)} dt - \alpha_1 X_{3(t+1)} dt + \sigma_{t+1} \varepsilon_{t+1} \end{aligned} \quad (9)$$

$$\begin{aligned} X_{1(t+3)} - X_{1(t+2)} &= X_{1(t+2)} dt + \sigma_{t+2} \varepsilon_{t+2} \\ X_{2(t+3)} - X_{2(t+2)} &= X_{3(t+2)} dt + \sigma_{t+2} \varepsilon_{t+2} \\ X_{3(t+3)} - X_{3(t+2)} &= -\alpha_3 X_{1(t+2)} dt - \alpha_2 X_{2(t+2)} dt - \alpha_1 X_{3(t+2)} dt + \sigma_{t+2} \varepsilon_{t+2} \end{aligned} \quad (10)$$

substituting into the X_1 dynamics:

$$\begin{aligned} X_{1(t+3)} &\approx (3 - \alpha_1) X_{1(t+2)} + (2\alpha_1 - \alpha_2 - 3) X_{1(t+1)} + (-\alpha_1 + \alpha_2 - \alpha_3 + 1) X_{1(t)} \\ &+ \sigma_t (B_{t-1} - B_t) \end{aligned} \quad (11)$$

For Berlin temperature we have identified $p = 3$, see Figure 2. The AR(3) is equal to

$$X_{t+3} = 0.91 X_{t+2} - 0.20 X_{t+1} + 0.07 X_t + \sigma_t \varepsilon_t$$

. The $CAR(3)$ -parameters are therefore $\alpha_1 = 2.09, \alpha_2 = 1.38, \alpha_3 = 0.22$. The stationarity condition is fulfilled, since the eigenvalues of A have negative real parts ($\lambda_1 = -0.2069, \lambda_{2,3} = -0.9359 \pm 0.3116i$). The element components of the matrix A do not change over time, what makes the process to be stable.

3 A pricing model

In this section we describe the construction of pricing Future/Option for different temperature contracts.

3.1 Temperature derivatives

Temperature derivatives are written on a temperature index. The most common weather indices on temperature are: Heating Degree Day (HDD), Cooling Degree Day (CDD), Cumulative Averages (CAT), Average of Average

Indices	Jan	Feb	March	April	May	Jun	Jul	Aug	Sept	Oct	Nov	Dec
CDD	0	0	0	0	28.3	42	71	23.3	24.9	0	0	0
HDD	472.8	526.4	471.4	241.1	150.2	71.8	24.8	43.9	73.5	199.5	398.2	525.8
CAT	103.2	-4.4	104.6	316.9	454.1	528.2	622.2	555.4	509.4	376.5	159.8	50.2
AAT	3.32	-0.15	3.37	10.56	14.64	17.60	20.07	17.91	16.98	12.14	5.32	1.61

Table 2: Degree day indices for temperature data (2005) Berlin.

Temperature (AAT) and Event Indices (EI), ?. The HDD index measures the temperature over a period $[\tau_1, \tau_2]$, usually between October to April, and it is defined as:

$$HDD(\tau_1, \tau_2) = \int_{\tau_1}^{\tau_2} \max(c - T_u, 0) du \quad (12)$$

where c is the baseline temperature (typically 18C or 65F) and T_u is the average temperature on day u . Similarly, the CDD index measures the temperature over a period $[\tau_1, \tau_2]$, usually between November and March, and it is defined as:

$$CDD(\tau_1, \tau_2) = \int_{\tau_1}^{\tau_2} \max(T_u - c, 0) du \quad (13)$$

The HDD and the CDD index are used to trade futures and options in 18 US cities (Atlanta, Des Moines, New York, Baltimore, Detroit, Philadelphia, Boston, Houston, Portland, Chicago, Kansas City, Sacramento, Cincinnati, Las Vegas, Salt Lake City, Dallas, Minneapolis-St. Paul, Tucson), 6 Canadian cities (Calgary, Edmonton, Montreal, Toronto, Vancouver and Winnipeg), 9 European cities (Amsterdam, Essen, Paris, Barcelona, London, Rome, Berlin, Madrid, Stockholm) and 2 Japanese cities (Tokyo and Osaka). The CAT index accounts the accumulated average temperature over a period $[\tau_1, \tau_2]$ days:

$$CAT(\tau_1, \tau_2) = \int_{\tau_1}^{\tau_2} T_u du \quad (14)$$

Since $\max(T_u - k, 0) - \max(K - T_u, 0) = T_u - k$, we get the HDD-CDD parity

$$CDD(\tau_1, \tau_2) - HDD(\tau_1, \tau_2) = CAT(\tau_1, \tau_2) - c(\tau_2 - \tau_1) \quad (15)$$

Therefore, it is sufficient to analyse only CDD and CAT indices. The AAT measures the "excess" or deficit of temperature i.e. the average of average temperatures over $[\tau_1, \tau_2]$ days:

$$AAT(\tau_1, \tau_2) = \frac{1}{\tau_1 - \tau_2} \int_{\tau_1}^{\tau_2} T_u du \quad (16)$$

This index is just the average of the CAT and it is relevant for the Pacific Rim consisting of two Japanese cities (Tokyo and Osaka). The EI considers the number of times a certain meteorological event occurs in the contract period. For example, a frost day is considered when the temperature at 7:00-10:00 local time is less than or equal to -3.5C. To illustrate this, Table 2 shows the expected number of HDDs, CDDs, CATs and AATs for Berlin temperature data.

In this paper, we will focus on the pricing of some of the most common temperature futures traded at the CME, i.e. monthly CAT, CDD and HDD indices. Table 3 described the CME - WD data from 20031003 - 20070521. The contract size of a future traded at CME is 20 pounds times the Degree Day Index (for convenience, we call it "price"). The minimum price increment is one Degree Day Index point. The degree day metric is Celsius and the tick value is twenty pounds. The termination of the trading is two calendar days following the expiration of the contract month. The Settlement is based on the relevant Degree Day index on the first exchange business day at least two calendar days after the futures contract month. The accumulation period of each CAT index futures contract begins with the first calendar day of the contract month and ends with the calendar day of the contract month. Earth Satellite Corporation reports to CME the daily average temperature. The notation used by CME for temperature futures is the following: F for January, G for February, H for March, J for April, K for May, M for June, N for July, Q for August, U for September, V for November and X for December. J7 stands for 2007, J8 for 2008, etc. The J7 contract corresponds to the month of April, i.e. the temperature measurement

Code	Trading-Period		Measurement-Period	
	First-trade	Last-trade	τ_1	τ_2
J7	20060503	20070502	20070401	20070430
K7	20060603	20070602	20070501	20070531
M7	20060705	20070702	20070601	20070630
N7	20060803	20070802	20070701	20070731
Q7	20060906	20070904	20070801	20070831
U7	20061003	20071002	20070901	20070930
V7	20061103	20071102	20071001	20071031
X7	20061204	20071202	20071101	20071130
Z7	20070104	20080102	20071201	20071231
F8	20080204	20080202	20080101	20080131
G8	20070304	20080302	20070201	20080228
H8	20070404	20080402	20070301	20080331

Table 3: Contracts listed at the CME. Source: Bloomberg

period was from 20070401 (τ_1) to 20070430 (τ_2) and started to be traded from 20060503 to 20070502. Figure 9 plots the values of Berlin CAT and HDD Future Prices traded on the 20060530 at the CME. Observe that seven contracts are traded for CAT futures (from April to October) and for HDD futures (from November to April). At the trading day t , one can buy contracts with measurement period $\tau_1 \leq t \leq \tau_2$ or $t < \tau_1 \leq \tau_2$ (six months ahead from the trading day t). The temperature future prices are very stable over time, as we see in Figure 10, where the CAT future prices from 20060417 to 20060530 are plotted. The prices are very high when the measurement period of temperature is August.

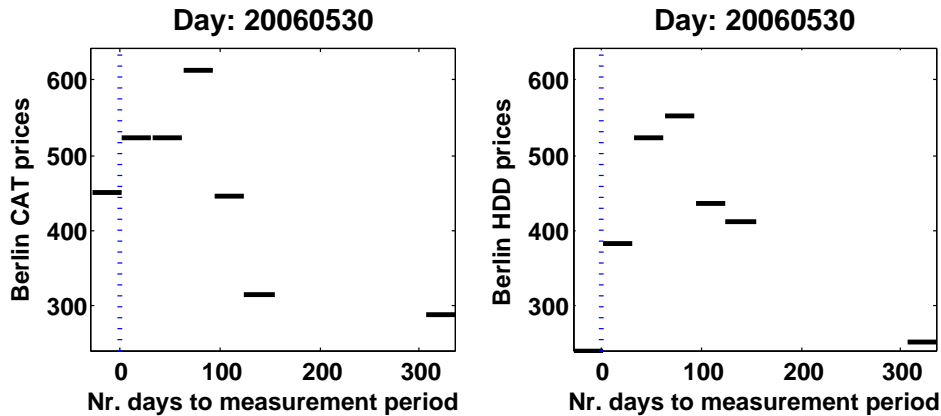


Figure 9: Berlin CAT/HDD Future Prices traded on the 20060530 at the CME. Source: Bloomberg

Figure 11 shows the plots of the Berlin CAT and HDD future prices with $\tau_1 < t \leq \tau_2$ from the period 2001 to 2006 reported by Bloomberg (red line), Earth Satellite Corporation (blue) and our estimates (black line). The average relative difference from the values reported from Bloomberg and Earth Satellite Corporation is equal to 2.43 for HDD prices and -10.57 for CAT prices. The average relative difference from our estimates and the values reported by Earth Satellite Corporation is equal to 0.04 for HDD prices and -0.09 for CAT prices.

3.2 Temperature futures pricing

As the temperature is not a tradable asset in the market, no replication arguments hold for any temperature futures and incompleteness of the market follows. In this context all equivalent measures Q will be risk-neutral probabilities. We assume the existence of an outstanding pricing measure Q , which can be parametrize and complete the market, ?. For that, we pinned down an equivalent measure $Q = Q_{\theta_t}$ to compute the arbitrage free price of a temperature future:

$$F_{(t, \tau_1, \tau_2)} = E^{Q_{\theta_t}} [Y_T(T_t) | \mathcal{F}_t] \quad (17)$$

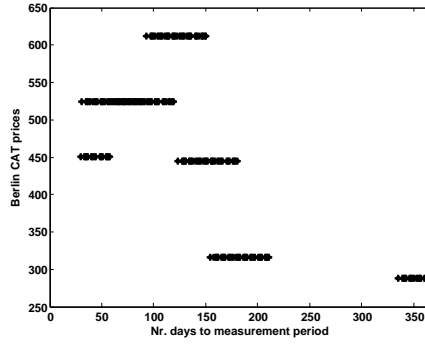


Figure 10: Berlin CAT Future Prices from 20060417 to 20060530. Source: Bloomberg

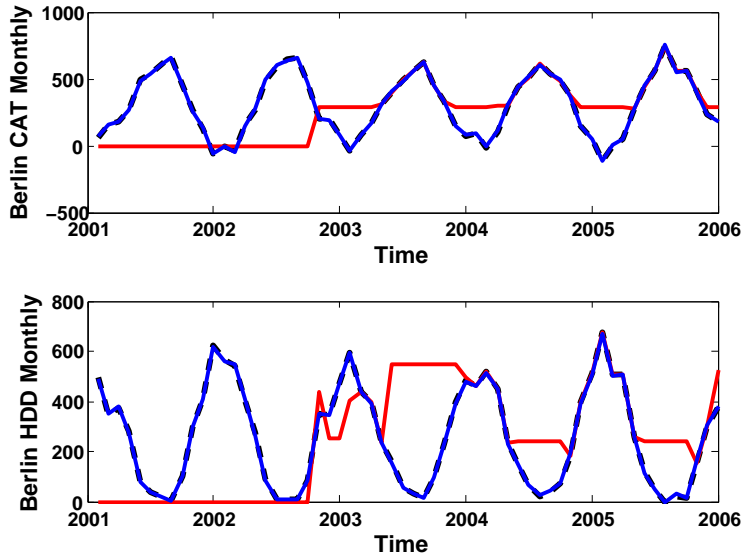


Figure 11: Berlin CAT/HDD Future Prices traded on the 20060530 at the CME. Source: Bloomberg

where Y_T is the payoff from the temperature index (CAT,HDD,CDD indices) at $T > t$ and θ_t denotes the time dependent market price of risk (MPR). By Girsanov theorem:

$$B_t^\theta = B_t - \int_0^t \theta_u du$$

is a Brownian motion for $t \leq \tau_{\max}$ and a martingale under Q_{θ_t} . ? proposed a θ_t (market price of risk) as a real valued, bounded and piecewise continuous function. In the next section, we relax that assumption, by considering (non)-time dependent market price of risk. In fact, from Theorem 4.2 (page 12) in ?, we can parametrize the market price of risk and relate θ_t to the risk premium by the equation

$$\mu t + \delta t - r_t \tilde{\mathbf{1}} = \sigma_t \theta_t \quad (18)$$

where $\tilde{\mathbf{1}}$ denotes the N-dimensional vector with every component equal to one, μ_t is the N-dimensional mean rate of return process, δt defines a N-dimensional dividend rate process, σ_t denotes the volatility process and r_t determines the risk-free interest rate process. For example, in the Black-Scholes Model framework, the asset price follows:

$$S_t = S_0 \exp \left[\left\{ \mu(S_t, t) - \frac{1}{2} \sigma^2(S_t, t) \right\} t + \sigma(S_t, t) B_t \right]$$

with $\frac{dS_t}{S_t} = \mu(S_t, t)dt + \sigma(S_t, t)dB_t$, where $t \in [0, T]$, B_t is standard Brownian motion under measure Q and by Girsanov theorem $B_t^\theta = B_t - \int_0^t \theta_u du$ is also Brownian motion under Q_{θ_t} for $t \leq \tau_{\max}$. It follows that the measure Q_{θ_t} is given by:

$$\frac{dQ_{\theta_t} |_{\mathcal{F}_t}}{dQ} = \exp \left(- \int_0^t \theta_u dB_u - \frac{1}{2} \int_0^t \theta_u^2 du \right)$$

where the market price of risk $\theta_t = (\mu_t - r_t)/\sigma_t$. Then, under Q_θ , the dynamics of the underlying process are:

$$\frac{dS_t}{S_t} = \{ \mu(S_t, t) + \sigma(S_t, t)\theta_t \} dt + \sigma(S_t, t)dB_t^\theta$$

Similarly, under Q^θ , the dynamics of equation (7) become

$$d\mathbf{X}_t = (A\mathbf{X}_t + \mathbf{e}_p \sigma_t \theta_t) dt + \mathbf{e}_p \sigma_t dB_t^\theta \quad (19)$$

with explicit dynamics, for $s \geq t \geq 0$:

$$\mathbf{X}_s = \exp \{ A(s-t) \} \mathbf{x} + \int_t^s \exp \{ A(s-u) \} \mathbf{e}_p \sigma_u \theta_u du + \int_t^s \exp \{ A(s-u) \} \mathbf{e}_p \sigma_u dB_u^\theta \quad (20)$$

Observe that the volatility σ_t from the econometric part is deterministic for every t, so that the relationship $\theta_t = (\mu_t - r_t)/\sigma_t$ between θ_t and σ_t is well identified.

3.2.1 CAT Futures/Option

Following equation (17), the risk neutral price of a future based on a CAT index is defined as:

$$F_{CAT(t, \tau_1, \tau_2)} = E^{Q^\theta} \left[\int_{\tau_1}^{\tau_2} T_s ds | \mathcal{F}_t \right] \quad (21)$$

For contracts whose trading date is earlier than the temperature measurement period, i.e. $0 \leq t \leq \tau_1 < \tau_2$, ? calculate the future price explicitly by inserting the temperature model (equation 4) into equation 21:

$$F_{CAT(t, \tau_1, \tau_2)} = \int_{\tau_1}^{\tau_2} \Lambda_u du + \mathbf{a}_{t, \tau_1, \tau_2} \mathbf{X}_t + \int_t^{\tau_1} \theta_u \sigma_u \mathbf{a}_{t, \tau_1, \tau_2} \mathbf{e}_p du + \int_{\tau_1}^{\tau_2} \theta_u \sigma_u \mathbf{e}_1^\top A^{-1} [\exp \{ A(\tau_2 - u) \} - I_p] \mathbf{e}_p du \quad (22)$$

with $\mathbf{a}_{t, \tau_1, \tau_2} = \mathbf{e}_1^\top A^{-1} [\exp \{ A(\tau_2 - t) \} - \exp \{ A(\tau_1 - t) \}]$ and $p \times p$ identity matrix I_p .

We observed from real data that the CME trades CAT futures between the temperature measurement period, i.e. $\tau_1 \leq t \leq \tau_2$. Following the same pricing methodology as before, we calculate the risk neutral price for this kind of contracts:

$$\begin{aligned} F_{CAT}(t, \tau_1, \tau_2) &= E^{Q^\theta} \left[\int_t^{\tau_2} T_s ds | \mathcal{F}_t \right] + E^{Q^\theta} \left[\int_{\tau_1}^t T_s ds | \mathcal{F}_t \right] \\ &= E^{Q^\theta} \left[\int_{\tau_1}^t T_s ds | \mathcal{F}_t \right] + \int_t^{\tau_2} \Lambda_u du + \mathbf{a}_{t, \tau_1, \tau_2} \mathbf{X}_t + \int_t^{\tau_2} \theta_u \sigma_u \mathbf{e}_1^\top A^{-1} [\exp \{A(\tau_2 - u)\} - I_p] \mathbf{e}_p du \end{aligned}$$

where $\mathbf{a}_{t, \tau_1, \tau_2} = \mathbf{e}_1^\top A^{-1} [\exp \{A(\tau_2 - t)\} - I_p]$. Notice that the expected value of the temperature from τ_1 to t is known.

? also calculate explicit formulas for the CAT call option written on a CAT future with strike K at exercise time $\tau < \tau_1$ during the period $[\tau_1, \tau_2]$:

$$\begin{aligned} C_{CAT}(t, \tau, \tau_1, \tau_2) &= \exp \{-r(\tau - t)\} \\ &\times \left[(F_{CAT}(t, \tau_1, \tau_2) - K) \Phi \{d(t, \tau, \tau_1, \tau_2)\} + \int_t^\tau \Sigma_{CAT}^2(s, \tau_1, \tau_2) ds \Phi \{d(t, \tau, \tau_1, \tau_2)\} \right] \quad (23) \end{aligned}$$

where $d(t, \tau, \tau_1, \tau_2) = \frac{F_{CAT}(t, \tau_1, \tau_2) - K}{\sqrt{\int_t^\tau \Sigma_{CAT}^2(s, \tau_1, \tau_2) ds}}$ and $\Sigma_{CAT}(s, \tau_1, \tau_2) = \sigma_t \mathbf{a}_{t, \tau_1, \tau_2} \mathbf{e}_p$ and Φ denotes the standard normal cdf.

To replicate the call option with CAT-futures, one should compute the number of CAT-futures held in the portfolio, which is simply computed by the option's delta:

$$\Phi \{d(t, T, \tau_1, \tau_2)\} = \frac{\partial C_{CAT}(t, \tau, \tau_1, \tau_2)}{\partial F_{CAT}(t, \tau_1, \tau_2)} \quad (24)$$

The strategy holds close to zero CAT futures when the option is far out of the money, close to 1 otherwise.

Figure 13 shows the volatility term structure of CAT temperature futures $\sigma_u \mathbf{a}_{t, \tau_1, \tau_2}$ presents a a Samuelson

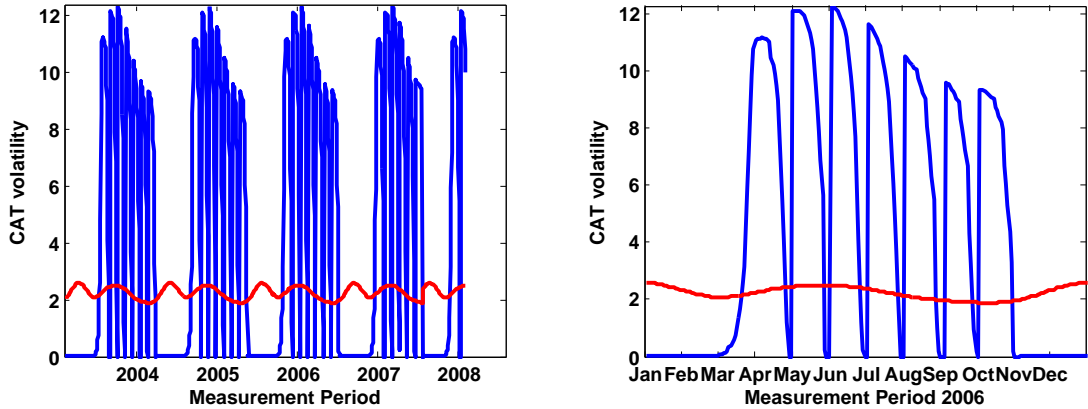


Figure 12: The Berlin CAT term structure of volatility from 2004-2008 (left side) and 2006 (right side) for contracts traded within the measurement period

effect, which is very common in future contract based on a mean reverting commodity price. In this effect, we observed that the volatility of temperature is decreasing with the time to delivery. The CAT future volatility is close to zero when the time to measurement is large, temperature deviations are smoothed over time. It increases up to the start of the measurement period. In Figure 14 we plot 2 contracts in March: one with measurement period of 1 month and the other of 1 week. The contract with the longest measurement period has the largest volatility. In both contracts, the effect of the CAR(3) can be observed when the volatility is decaying just before maturity of the contracts. The later effect together with the Samuelson effect on Berlin CAT futures are also similar for Stockholm CAT futures ?, however the deviations are less smoothed for Berlin.

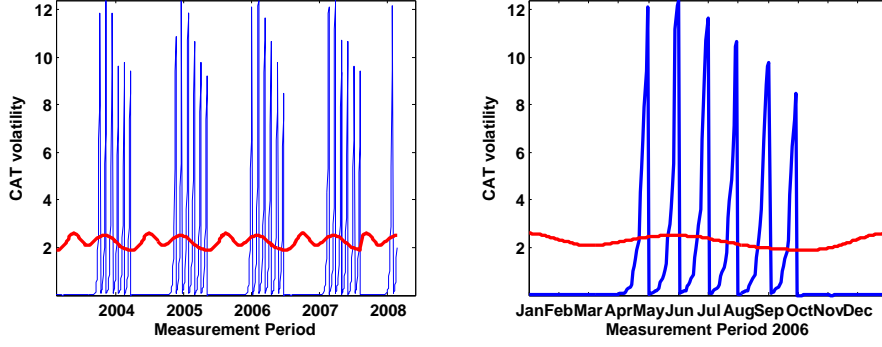


Figure 13: The Berlin CAT term structure of volatility from 2004-2008 (left side) and 2006 (right side) for contracts traded before the measurement period

3.2.2 CDD Futures/Options

Analogously, ? derived explicit the CDD future price. Following equation (17), the risk neutral price of a CDD future which is traded at $0 \leq t \leq \tau_1 < \tau_2$ is defined as:

$$\begin{aligned}
 F_{CDD(t, \tau_1, \tau_2)} &= E^{Q_\theta} \left[\int_{\tau_1}^{\tau_2} \max(T_s - c, 0) ds | \mathcal{F}_t \right] \\
 &= \int_{\tau_1}^{\tau_2} v_{t,s} \psi \left[\frac{m_{\{t,s, \mathbf{e}_1^\top \exp\{A(s-t)\} \mathbf{X}_t\}} - c}{v_{t,s}} \right] ds
 \end{aligned} \quad (25)$$

where $m_{\{t,s,x\}} = \Lambda_s - c + \int_t^s \sigma_u \theta_u \mathbf{e}_1^\top \exp\{A(s-t)\} \mathbf{e}_p du + x$, $v_{t,s}^2 = \int_t^s \sigma_u^2 [\mathbf{e}_1^\top \exp\{A(s-t)\} \mathbf{e}_p]^2 du$ and $\psi(x) = x\Phi(x) + \varphi(x)$ with $x = \mathbf{e}_1^\top \exp\{A(s-t)\} \mathbf{X}_t$.

For CDD futures contracts traded at $\tau_1 \leq t \leq \tau_2$, the non-arbitrage price of a CDD future is:

$$\begin{aligned}
 F_{CDD(t, \tau_1, \tau_2)} &= E^{Q_\theta} \left[\int_{\tau_1}^{\tau_2} \max(T_s - c, 0) ds | \mathcal{F}_t \right] \\
 &= E^{Q_\theta} \left[\int_{\tau_1}^t \max(T_s - c, 0) ds | \mathcal{F}_t \right] + \int_t^{\tau_2} v_{t,s} \psi \left[\frac{m_{\{t,s, \mathbf{e}_1^\top \exp\{A(s-t)\} \mathbf{X}_t\}} - c}{v_{t,s}} \right] ds
 \end{aligned} \quad (26)$$

with $m_{\{t,s,x\}}$ and $v_{t,s}^2$ defined as above. Notice again that the expected value of the temperature from τ_1 to t is known. For the call option written CDD-future, ? found no analytical solution, but an expression suitable for Monte Carlo simulation. The risk neutral price of a CDD call written on a CDD future with strike K at exercise time $\tau < \tau_1$ during the period $[\tau_1, \tau_2]$:

$$\begin{aligned}
 C_{CDD(t, T, \tau_1, \tau_2)} &= \exp\{-r(\tau - t)\} \\
 &\times E \left[\max \left(\int_{\tau_1}^{\tau_2} v_{\tau,s} \psi \left(\frac{m_{\text{index}} - c}{v_{\tau,s}} \right) ds - K, 0 \right) \right]_{\mathbf{x}=\mathbf{X}_t}
 \end{aligned} \quad (27)$$

where $\text{index} = \tau, s, \mathbf{e}_1^\top \exp\{A(s-t)\} \mathbf{x} + \int_t^\tau \mathbf{e}_1^\top \exp\{A(s-u)\} \mathbf{e}_p \sigma_u \theta_u du + \Sigma_{s,t,\tau} Y$, $Y \sim N(0, 1)$ and $\Sigma_{s,t,\tau}^2 = \int_t^\tau [\mathbf{e}_1^\top \exp\{A(s-u)\} \mathbf{e}_p]^2 \sigma_u^2 du$.

4 Inferring the market price of temperature risk

The incompleteness of the WD market requires the estimation of the market price of weather risk (MPR) for pricing and hedging temperature derivatives. The MPR adjusts the underlying process so that the level the risk aversion is not needed for valuation. In this part of the paper, we infer the market price of risk θ_t from Berlin monthly CAT temperature futures data traded at the CME. We thus know the MPR for temperature futures,

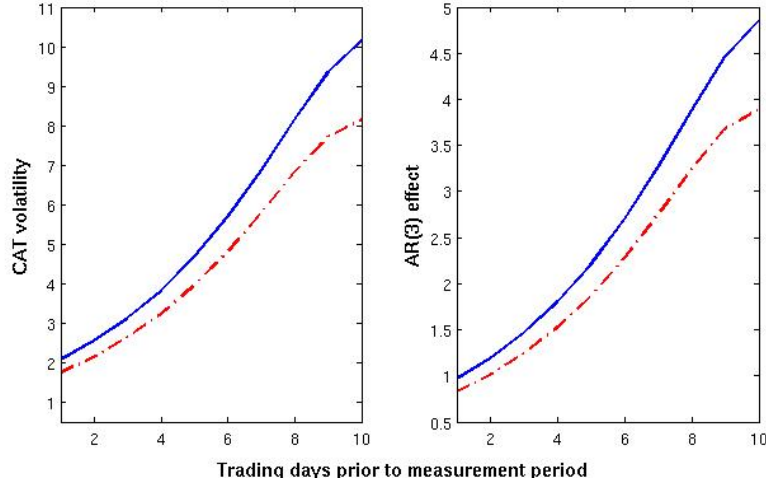


Figure 14: Berlin CAT volatility prior and AR(3) effect of 2 contracts in March 2007: one with measurement period of 1 month (blue line) and the other of 1 week (red line)

and hence we know the MPR for options. Moreover with this inferred information, we can price new derivatives, e.g. non standard contracts with "crazy maturities". We first study the contracts which are traded before the measurement period, i.e. $t < \tau_1 \leq \tau_2$ (or contract number $i = 2 \dots 7$), since their pricing value depends only on the expected value of the underlying process, while for the other contracts traded during the measurement period, i.e. $\tau_1 < t \leq \tau_2$ (or contract number $i = 1$), a partial or full information of the temperature development inside the measurement period is already known. Then, we mix both cases to study the dynamics of the MPR, when this one is assumed to be piecewise constant linear function or time dependent.

4.1 Constant market price of risk for each contract per trading day

From equation (22), we can infer θ_t for contracts with $t < \tau_1 \leq \tau_2$. Our first assumption is to set $\hat{\theta}_t$ as a constant for each of the i contract, with $i = 2 \dots 7$. $\hat{\theta}_t$ can be found solving the following inverse problem:

$$\arg \min_{\hat{\theta}_t} \left(F_{CAT}(t, \tau_1, \tau_2) - \int_{\tau_1}^{\tau_2} \hat{\Lambda}_u du - \hat{\mathbf{a}}_{t, \tau_1, \tau_2} \mathbf{X}_t - \hat{\theta}_t \left\{ \int_t^{\tau_1} \hat{\sigma}_u \hat{\mathbf{a}}_{t, \tau_1, \tau_2} \mathbf{e}_p du + \int_{\tau_1}^{\tau_2} \hat{\sigma}_u \mathbf{e}_1^\top A^{-1} [\exp \{A(\tau_2 - u)\} - I_p] \mathbf{e}_p du \right\} \right)^2 \quad (28)$$

The right upper part of Figure 17 shows the MPR estimates for each contract per trading day for Berlin CAT Future Prices traded on the 20060530 at the CME. The

4.2 Constant market price of risk per trading day

With least squares minimization method, the constant θ_t for all contracts with $t < \tau_1 \leq \tau_2$ at time t can be found:

$$\arg \min_{\hat{\theta}_t} \sum_{i=2}^7 \left(F_{CAT}(t, \tau_1^i, \tau_2^i) - \int_{\tau_1^i}^{\tau_2^i} \hat{\Lambda}_u du - \hat{\mathbf{a}}_{t, \tau_1^i, \tau_2^i} \mathbf{X}_t - \hat{\theta}_t \left\{ \int_t^{\tau_1^i} \hat{\sigma}_u \hat{\mathbf{a}}_{t, \tau_1^i, \tau_2^i} \mathbf{e}_p du + \int_{\tau_1^i}^{\tau_2^i} \hat{\sigma}_u \mathbf{e}_1^\top A^{-1} [\exp \{A(\tau_2^i - u)\} - I_p] \mathbf{e}_p du \right\} \right)^2 \quad (29)$$

4.3 2 constant market price of risk per trading day

Assuming now that, instead of one constant market price of risk per trading day, $\hat{\theta}_t = I(u \leq \xi) \hat{\theta}_t^1 + I(u > \xi) \hat{\theta}_t^2$ constant for all contracts i at time $t < \tau_1 \leq \tau_2$ and with breaking point ξ (take e.g. the first 150 days before the beginning of the measurement period). Then the inverse problem can be seen as a piecewise continuous function:

$$\begin{aligned}
 f(\xi) &= \arg \min_{\hat{\theta}_t^1, \hat{\theta}_t^2, \xi} \sum_{i=2}^7 \left(F_{CAT}(t, \tau_1^i, \tau_2^i) - \int_{\tau_1^i}^{\tau_2^i} \hat{\Lambda}_u du - \hat{\mathbf{a}}_{t, \tau_1^i, \tau_2^i} \mathbf{X}_t \right. \\
 &- \hat{\theta}_t^1 \left\{ \int_t^{\tau_1^i} I(u \leq \xi) \hat{\sigma}_u \hat{\mathbf{a}}_{t, \tau_1^i, \tau_2^i} \mathbf{e}_p du + \int_{\tau_1^i}^{\tau_2^i} I(u \leq \xi) \hat{\sigma}_u \mathbf{e}_1^\top A^{-1} [\exp \{A(\tau_2^i - u)\} - I_p] \mathbf{e}_p du \right\} \\
 &- \left. \hat{\theta}_t^2 \left\{ \int_t^{\tau_1^i} I(u > \xi) \hat{\sigma}_u \hat{\mathbf{a}}_{t, \tau_1^i, \tau_2^i} \mathbf{e}_p du + \int_{\tau_1^i}^{\tau_2^i} I(u > \xi) \hat{\sigma}_u \mathbf{e}_1^\top A^{-1} [\exp \{A(\tau_2^i - u)\} - I_p] \mathbf{e}_p du \right\} \right)^2 \quad (30)
 \end{aligned}$$

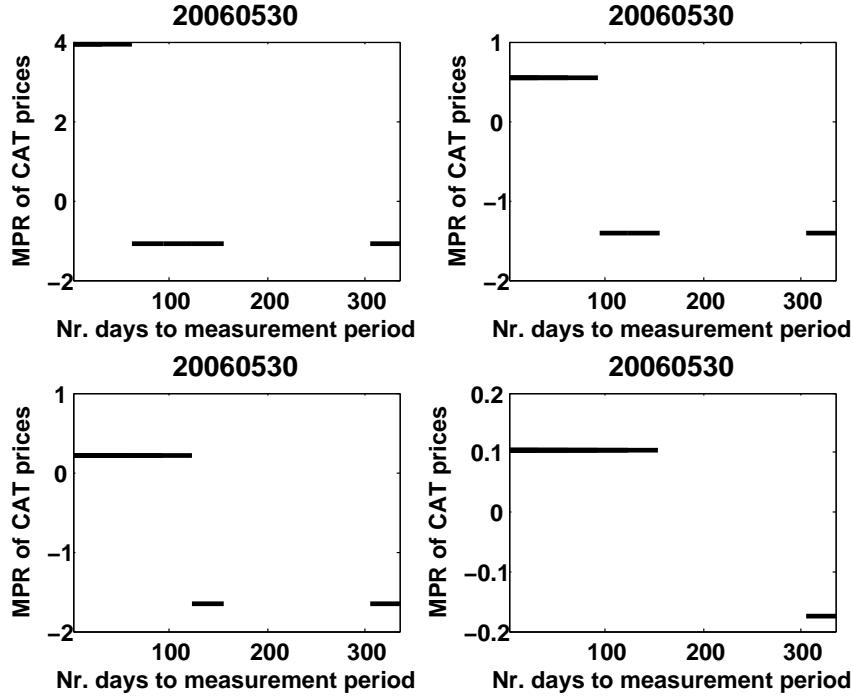


Figure 15: 2 constant MPR with $\xi = 62, 93, 123, 154$ days (upper left, upper right, lower left, lower right) for contracts with trading day 20060530 before the measurement period

The value of $\hat{\theta}_t^1$ and $\hat{\theta}_t^2$ can be obtained with least squares minimization method. The lower left part of Figure 17 shows the MPR estimates with $\xi = 150$ days for Berlin CAT Future Prices traded on the 20060530 at the CME. We notice that the value of the MPR decreases when the value of ξ increases, i.e. when the time to measurement period is getting large. This effect could be related to the Samuelson effect, where the volatility for each contract is close to zero when the time to measurement period is large. The optimal value of ξ was chosen such as $f(\xi)$ (the sum of the squared errors) is minimized. For $\xi = 62, 93, 123, 154$ days, the corresponding sum of squared errors are 2759, 14794, 15191 and 15526. Figure 15 shows the MPR estimates for different values of ξ of Berlin CAT Future Prices traded on the 20060530 at the CME, a date before the measurement period. Figure 16 shows the same situation as before but now all kind of contracts are considered, i.e. the contracts trading dates are in and before the measurement period.

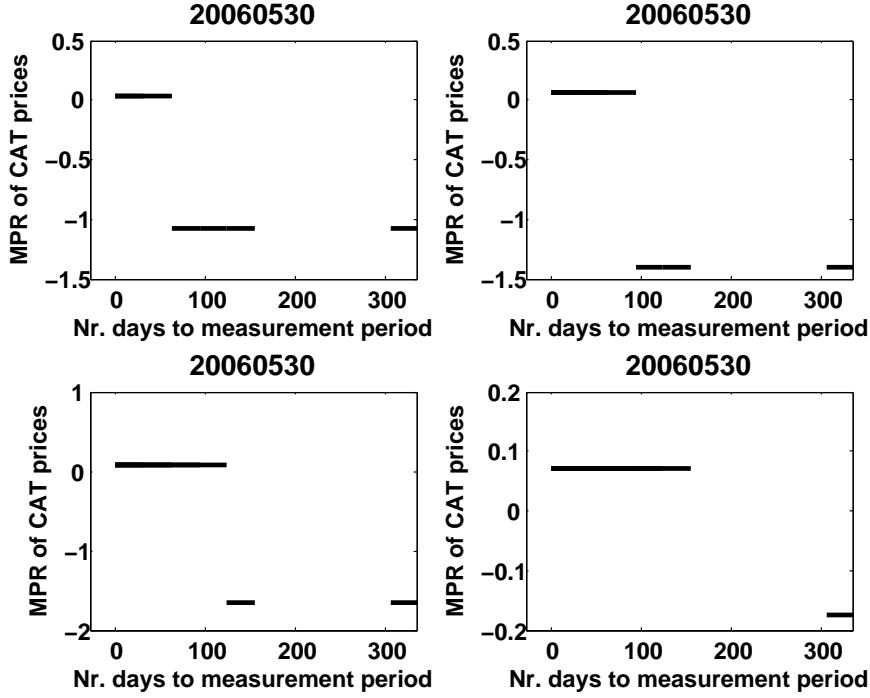


Figure 16: 2 constant MPR with $\xi = 62, 93, 123, 154$ days (upper left, upper right, lower left, lower right) for contracts with trading day 20060530 in and before the measurement period

4.4 General form of the market price of risk per trading day

The piecewise continuous function given in the previous subsection is just a particular case of a general form. Assume now that the MPR is dependent on time, then the inverse problem can be set as:

$$\arg \min_{\gamma_k} \sum_{i=2}^7 \left(F_{CAT}(t, \tau_1^i, \tau_2^i) - \int_{\tau_1^i}^{\tau_2^i} \hat{\Lambda}_u du - \hat{\mathbf{a}}_{t, \tau_1^i, \tau_2^i} \hat{\mathbf{X}}_t - \int_t^{\tau_1^i} \sum_{k=1}^K \hat{\gamma}_k \hat{h}_k(u_i) \hat{\sigma}_{u_i} \hat{\mathbf{a}}_{t, \tau_1, \tau_2} \mathbf{e}_p du_i - \int_{\tau_1^i}^{\tau_2^i} \sum_{k=1}^K \hat{\gamma}_k \hat{h}_k(u_i) \hat{\sigma}_{u_i} \mathbf{e}_1^\top A^{-1} [\exp \{A(\tau_2^i - u_i)\} - I_p] \mathbf{e}_p du_i \right)^2 \quad (31)$$

where $h_k(u_i)$ is a vector of known basis functions and γ_k defines the coefficients. One can obtain $h_k(u_i)$ with splines or polynomials. The right lower part of Figure 17 shows the MPR per trading day for Berlin CAT Future Prices traded on the 20060530 at the CME using cubic polynomials with number of knots equal to the number of traded contracts (6). The spline MPR is closed to zero, but then it explodes for the days when there is no trading.

4.5 Bootstrapping market price of risk

The bootstrap method can be applied to get estimates of the MPR for contracts with trading date earlier than the measurement period. If six contracts are traded at time $t < \tau_1^i \leq \tau_2^i$ with $i = 2 \dots 7$ and $\tau_1^i < \tau_1^{i+1} \leq \tau_2^i < \tau_2^{i+1}$, the resampling idea method consists on the estimation of $\hat{\theta}_1^i$ from the first contract ($i = 2$):

$$\arg \min_{\hat{\theta}_t^1} \left(F_{CAT}(t, \tau_1^2, \tau_2^2) - \int_{\tau_1^2}^{\tau_2^2} \hat{\Lambda}_u du - \hat{\mathbf{a}}_{t, \tau_1^2, \tau_2^2} \mathbf{X}_t - \right)$$

In similar way, the estimation of $\hat{\theta}_t^4, \hat{\theta}_t^5, \hat{\theta}_t^6$ can be obtained. The estimates of the bootstrap MPR lead to full replication of the CAT futures prices, like in the case when the MPR is constant per trading day. Table...

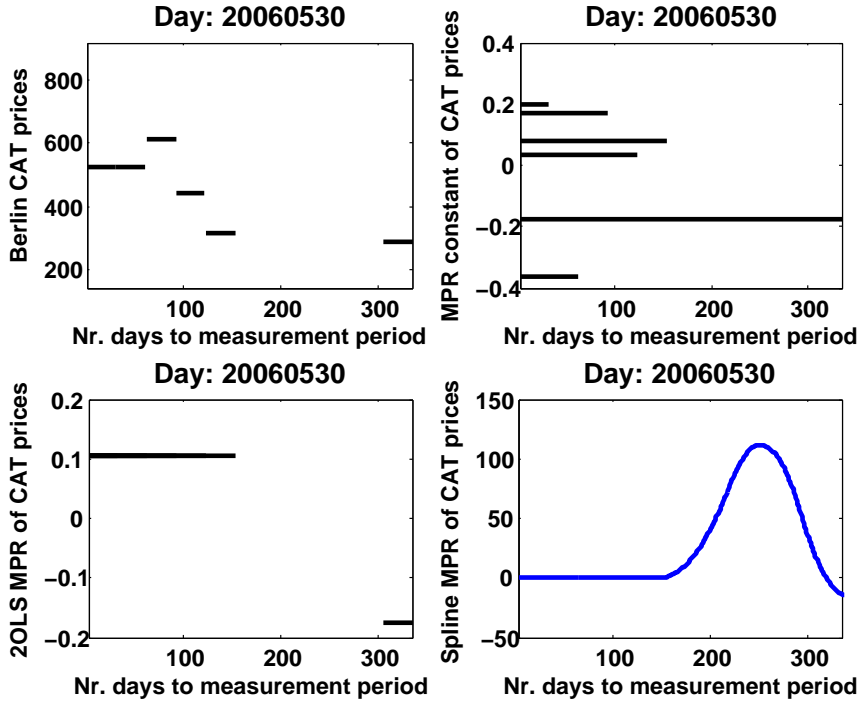


Figure 17: Prices (upper left) and MPR for Berlin CAT Futures traded on the 20060530 at the CME. Constant MPR for each contract per trading day (upper right), 2 constant MPR per trading day (lower left) and time dependent MPR using spline (lower right).

Figure 18 shows the box plot per CAT future contract type of the MPR estimates when this one is assumed to be constant per contract per trading day, constant per trading day (OLS), 2 constants per trading day (OLS2), Bootstrap and time dependent (represented by the Spline MPR). The data includes the MPR estimates from 20060501 to 20060530. Observe that in most of the cases, the median and mean of the MPR per contract i is negative, meaning that the producers are expected to pay lower price for the purchase of a temperature derivative. However, one can notice that in some days of contract 2,3,6 and 7, the MPR is positive, indicating the existence of consumers, who consider the temperature derivatives as a kind of insurance. Analogously, in Figure 19 shows that the relative differences between MPR estimates are more visible over contract type and depend on the current level of the constant MPR per contract per trading day. For example, the difference between the spline MPR and the constant MPR per trading day is equal to the absolute value of the difference divided by the value of the constant MPR. The MPR estimates obtained with the least squared minimization procedure show the highest relative difference with respect to the constant MPR.

4.6 Smoothing the market price of risk over time

After computing the MPR ($\hat{\theta}_t$) for each of the trading days for different contracts, a smoothing of the MPR with the inverse problem points can be made to find a MPR ($\hat{\theta}_u$) for every day (calendar and trading day) and with one can price temperature derivative for any maturity. We performed two procedures. The first one consisted on smoothing the MPR that was estimated in the previous subsection, i.e:

$$\arg \min_{f \in \mathcal{F}_j} \sum_{t=1}^n \left\{ \hat{\theta}_t - f(u_t) \right\}^2 = \arg \min_{\alpha_j} \sum_{t=1}^n \left\{ \hat{\theta}_t - \sum_{j=1}^6 \alpha_j \Psi_j(u_t) \right\}^2 \quad (33)$$

where $\Psi_j(u_t)$ is a vector of known basis functions, α_j defines the coefficients and $u_t = t + \Delta - 1$. In our case $u_t = 1$ day and $\Psi_j(u_t)$ is estimated using cubic splines. Figure 20, Figure 21 and Figure 22 show the smoothing of 1, 5 and 30 days of the constant MPR per contract per day (upper left), the constant MPR per day (upper right), the 2 constant MPR per day (middle left), the Bootstrap MPR (middle right) and the Spline MPR (lower left) for Berlin CAT Future traded on the 20060530 at the CME.

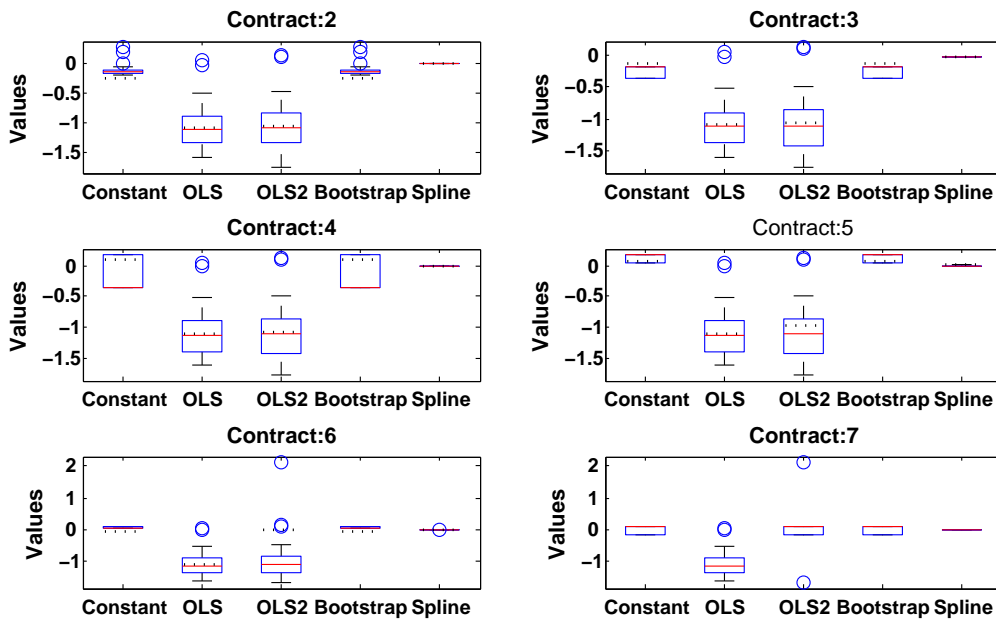


Figure 18: Box plot per CAT future contract type of the MPR estimates (20060501- 20060530) when this one is constant per contract per trading day, constant per trading day (OLS), 2 constants per trading day (OLS2), Bootstrap and smooth by Spline.

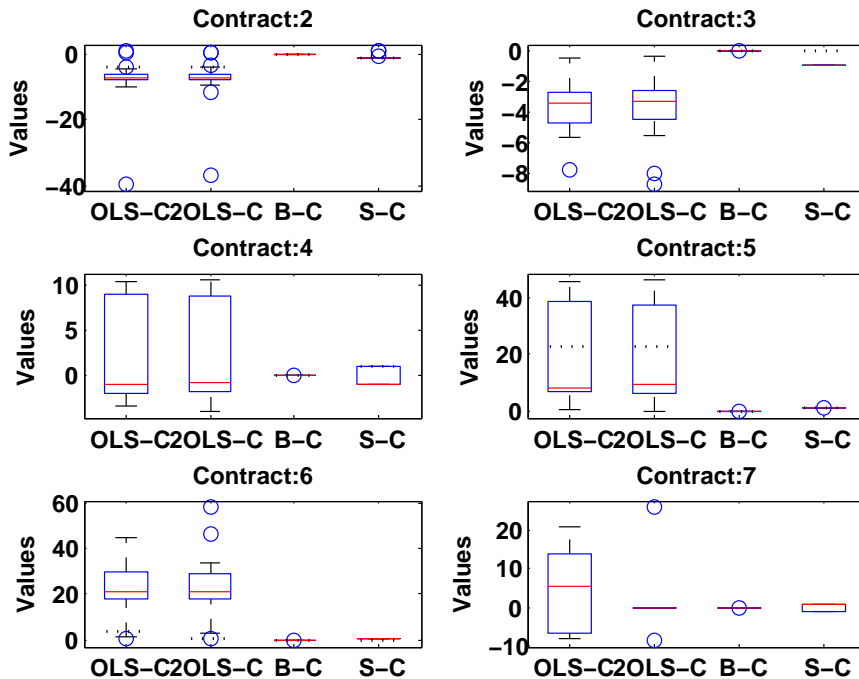


Figure 19: Box plot per CAT future contract type of the relative differences (20060501- 20060530) between MPR estimates: MPR constant per contract per trading day (C), MPR constant per trading day (OLS), 2 MPR constant per trading day (2OLS), Bootstrap MPR (B), Spline MPR (S).

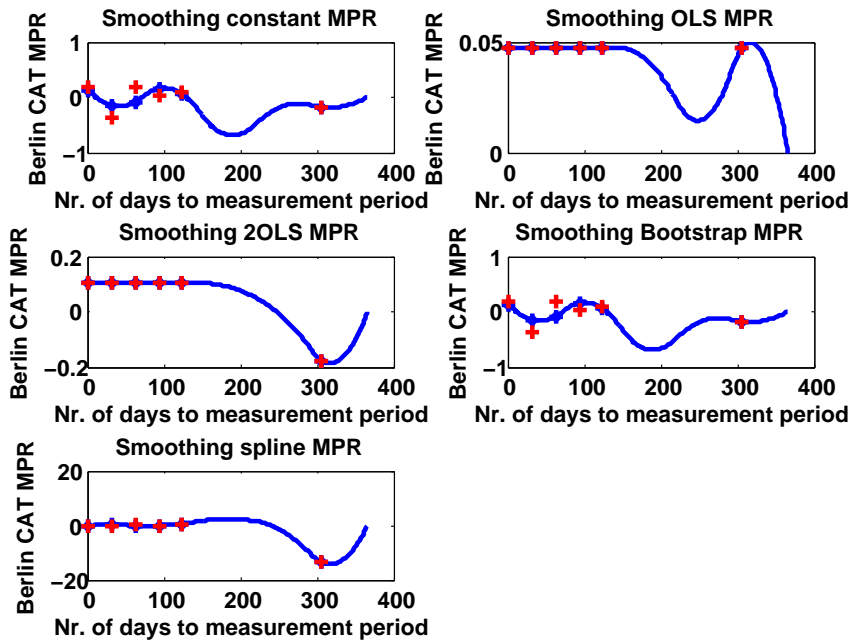


Figure 20: Smoothing 1 day: the constant MPR per contract per day (upper left), the constant MPR per day (upper right), the 2 constant MPR per day (middle left), the Bootstrap MPR (middle right) and the Spline MPR (lower left) for Berlin CAT Future traded on the 20060530 at the CME.

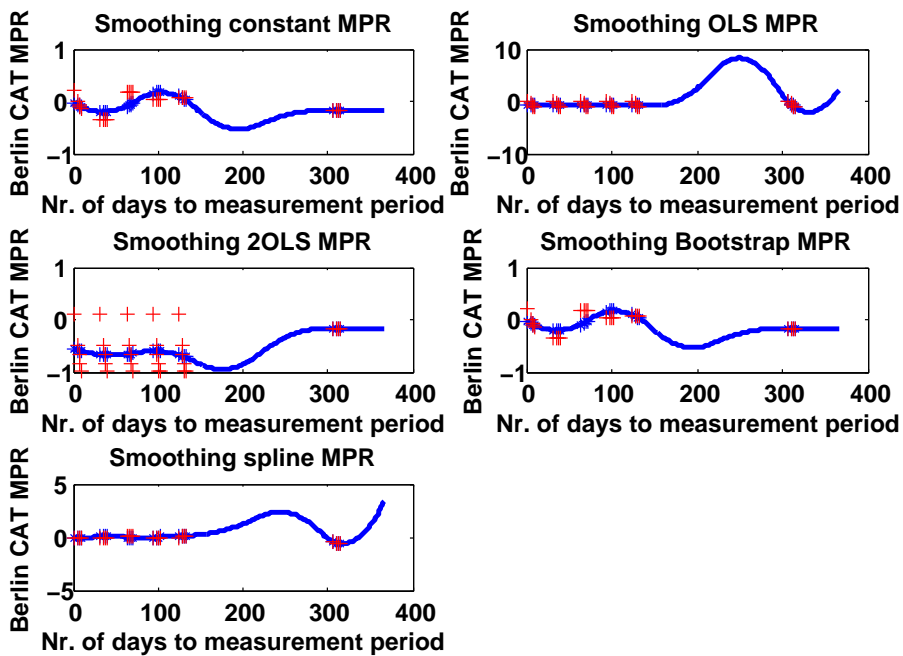


Figure 21: Smoothing 5 days: the constant MPR per contract per day (upper left), the constant MPR per day (upper right), the 2 constant MPR per day (middle left), the Bootstrap MPR (middle right) and the Spline MPR (lower left) for Berlin CAT Future traded on the 20060530 at the CME.

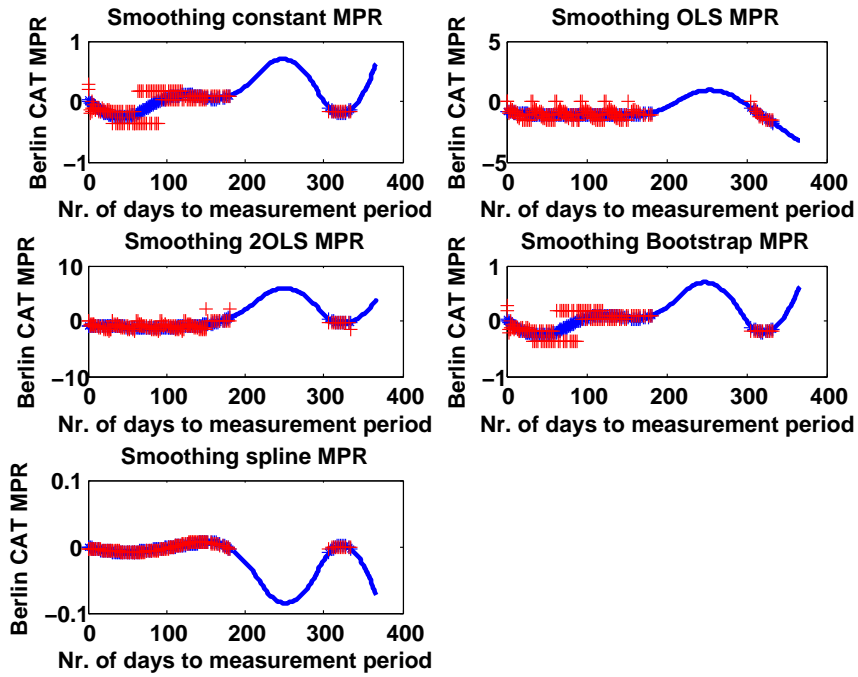


Figure 22: Smoothing 30 days: the constant MPR per contract per day (upper left), the constant MPR per day (upper right), the 2 constant MPR per day (middle left), the Bootstrap MPR (middle right) and the Spline MPR (lower left) for Berlin CAT Future traded on the 20060530 at the CME.

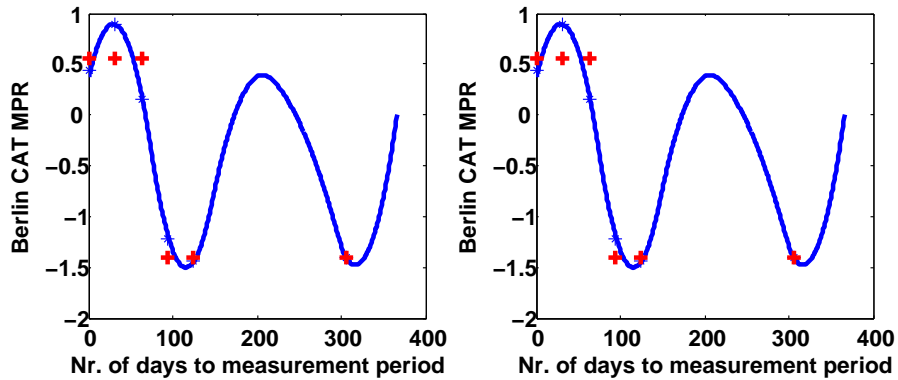


Figure 23: 1 day smooth of the MPR (left side) and of Berlin CAT prices for 5 lags: 20060522 to 20060530 (red crosses) and smoothed MPR of Berlin CAT prices for 5 lags (blue line with blue crosses)

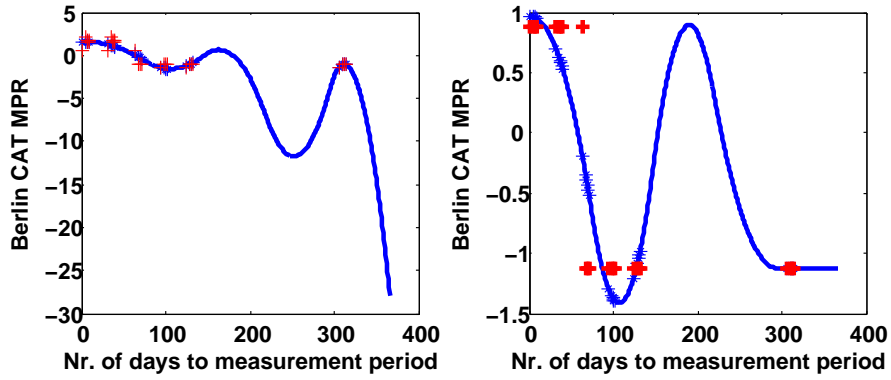


Figure 24: 5 days MPR of Berlin CAT prices for 30 lags: 20060522 to 20060530 (red crosses) and smoothed MPR of Berlin CAT prices for 5 lags (blue line with blue crosses)

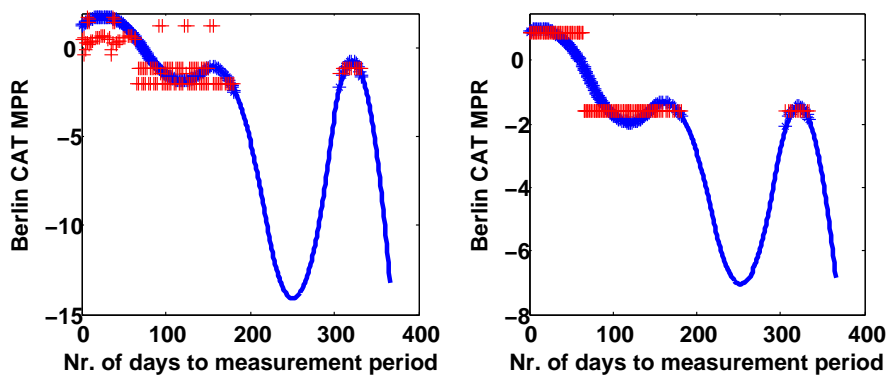


Figure 25: 30 days MPR of Berlin CAT prices for 30 lags: 20060522 to 20060530 (red crosses) and smoothed MPR of Berlin CAT prices for 5 lags (blue line with blue crosses)

4.7 Pricing CAT-HDD futures

The Chicago Mercantile exchange does not do trade CDD futures for Berlin, however the estimates of the smoothed MPR of CAT futures can be used to CDD futures, according to equation 22 or equation 26. Using the corresponding MPR's from last section, the left side of Figure 26 shows the estimated CAT future prices and the real prices extracted from Bloomberg (black line) for contracts traded before the measurement period. The estimates when the CAT future prices are very similar to the Bloomberg ones (black line) when the estimate of the MPR is constant per contract per trading day. The seasonality effect of the temperature is clearly reflected in the CAT future prices, high prices from June to August and low prices from September to April. When the estimations use smoothed MPR's, the effect is smoothed over time, see right side of Figure 26.

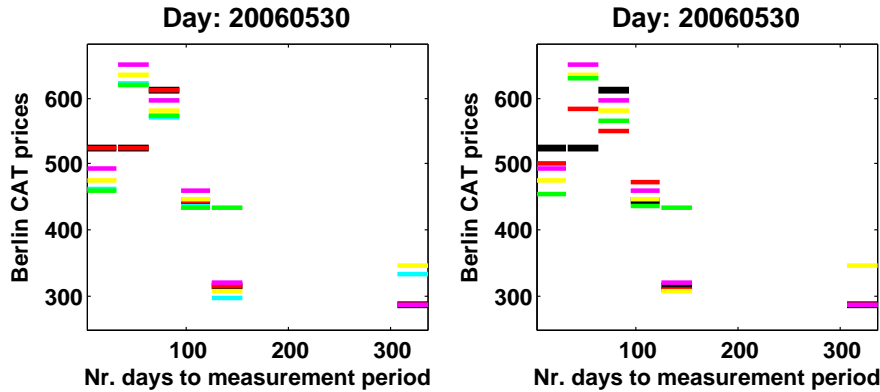


Figure 26: Right Side: Berlin CAT Future Prices from Bloomberg (black line) and estimated with constant MPR per contract per day (red line), MPR=0 (cyan line), constant MPR for all contracts (yellow line), 2 constant MPR per day (magenta line), Spline MPR(green line). Left Side: CAT Future Prices estimates using smoothed MPR's

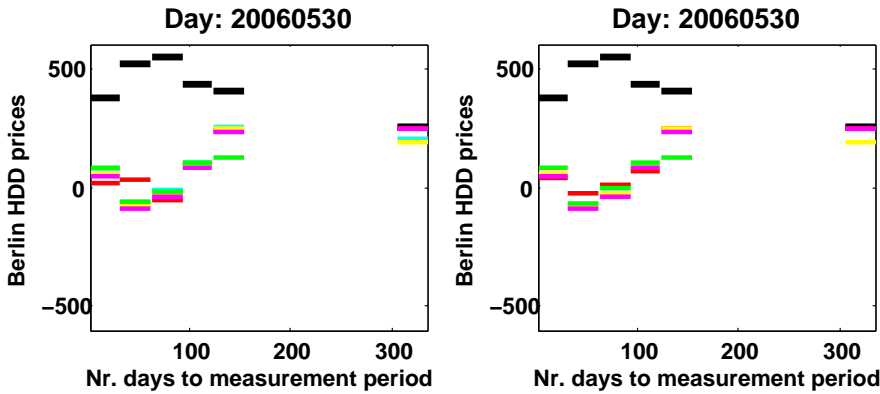


Figure 27: Right Side: Berlin HDD Future Prices from Bloomberg (black line) and estimated with constant MPR per contract per day (red line), MPR=0 (cyan line), constant MPR for all contracts (yellow line), 2 constant MPR per day (magenta line), Spline MPR(green line). Left Side: HDD Future Prices estimates using smoothed MPR's)

We also estimate the CAT futures prices for contracts traded during the measurement period. The prices also show a seasonal pattern, confirming the idea that most of the derivative price is driven by the seasonal effect. Figure 33 shows the estimated CAT future prices and the real prices extracted from Bloomberg (black line) for contracts traded in and before the measurement period.

5 Conclusion

We apply a higher order continuous-time autoregressive models CAR(3) with seasonal variance for modelling temperature in Berlin for more than 57 years of daily observations.

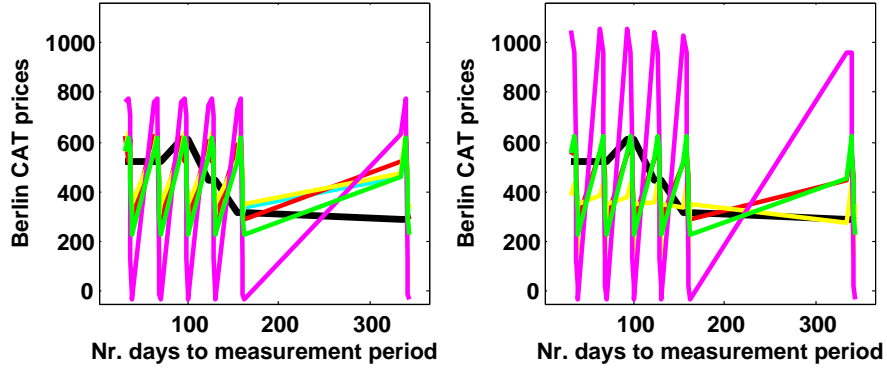


Figure 28: Right side: Berlin CAT Future Prices estimated with $MPR \neq 0$ (black line), $MPR = 0$ (magenta line), constant MPR for all contracts (red line). Left side: Estimates using smooth MPR

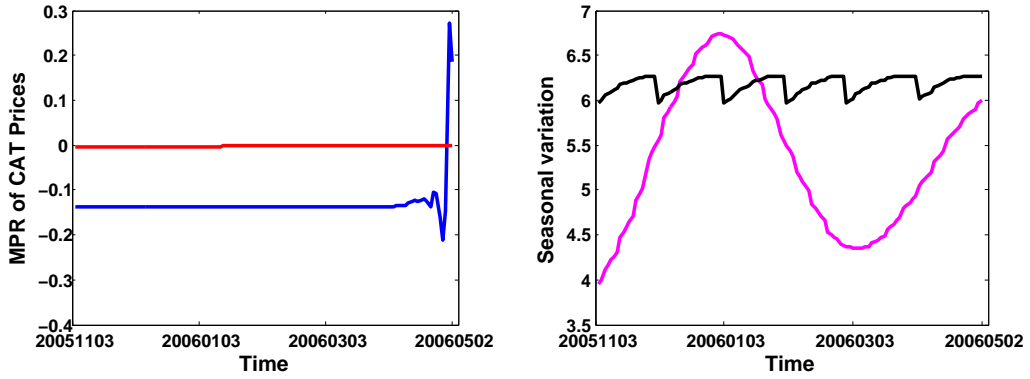


Figure 29: Left: Constant MPR $\hat{\theta}_t^i$ (blue)/smooth MPR $\hat{\theta}_t$ (red). Right: Seasonal Variation $\hat{\sigma}_{t+\Delta}^2$ (black) and $\hat{\sigma}_t^2$ (magenta) (right side) for Berlin CAT Future Prices, measurement period May 2006 (Contract K6)

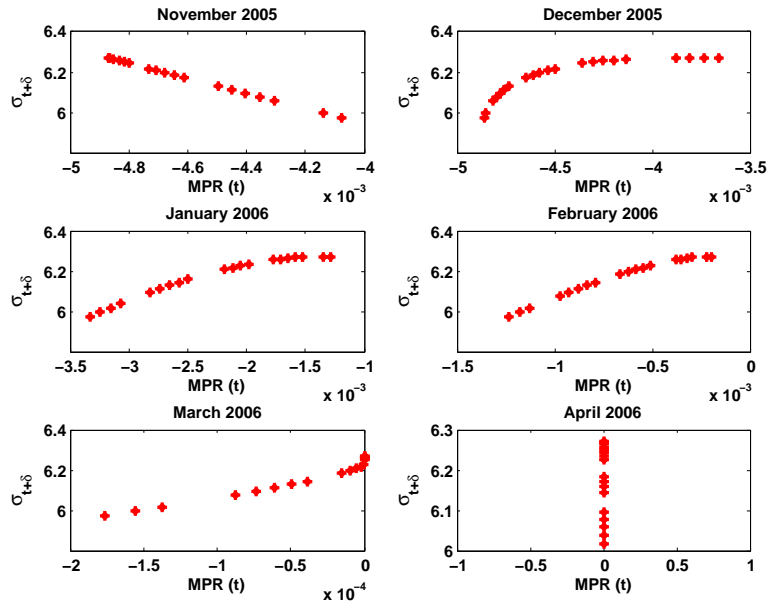


Figure 30: Seasonal Variation $\hat{\sigma}_{t+\Delta}^2$ and smoothed MPR $\hat{\theta}_t$ for Berlin CAT Future Prices 2006, measurement period May 2006 (Contract K6)

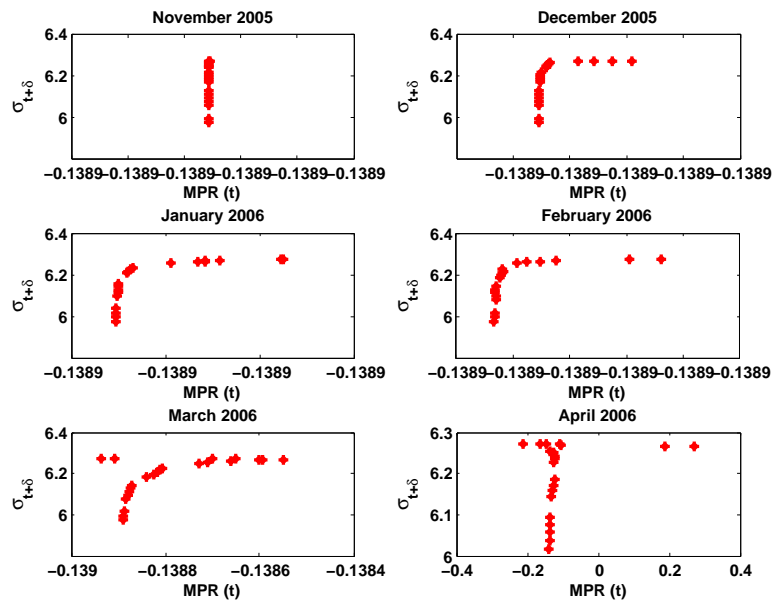


Figure 31: Seasonal Variation $\hat{\sigma}_{t+\Delta}^2$ and constant MPR $\hat{\theta}_t^i$ for Berlin CAT Future Prices, measurement period May 2006 (Contract K6)

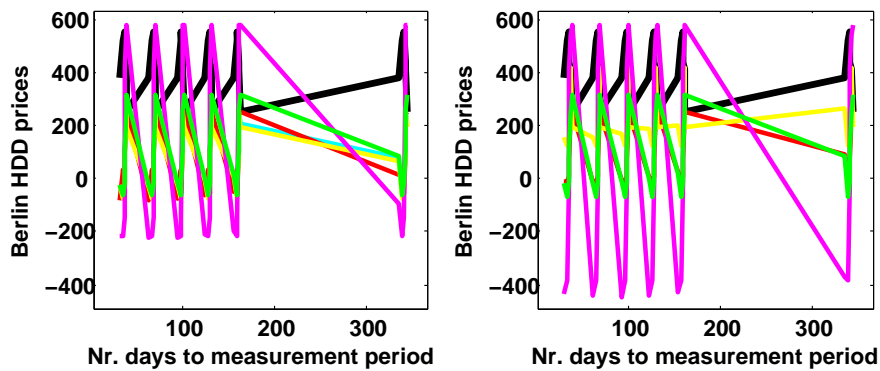


Figure 32: Berlin HDD Future Prices obtained from Bloomberg (black line) and estimated with MPR \neq 0 (blue line), MPR=0 (magenta line), constant MPR for all contracts (red line). Left side: Estimates using smooth MPR.

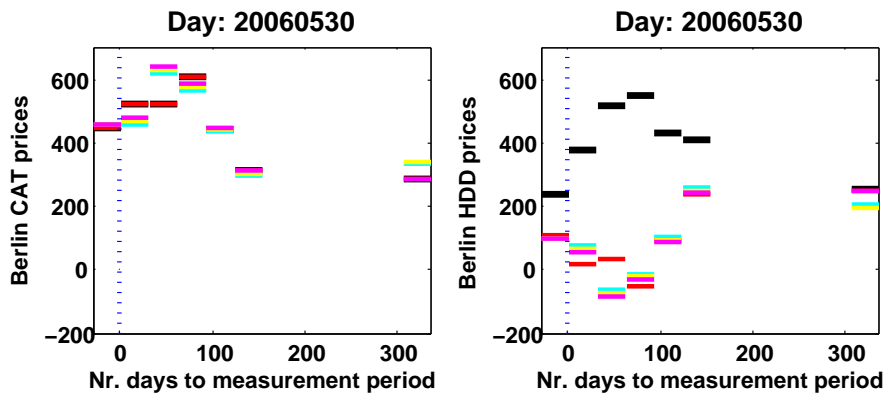


Figure 33: Berlin CAT-HDD Future Prices from Bloomberg (black line) and estimated with constant MPR per contract per day (red line), MPR=0 (cyan line), constant MPR for all contracts (yellow line), 2 constant MPR per day (magenta line), Spline MPR (green line)

This paper also analyze the weather options/future products for Berlin traded at the Chicago Mercantile Exchange (CME). We implied the market price of risk for Berlin CAT monthly temperature futures, which is different from zero. We study the seasonal structure of the market price of risk, not only as a piecewise constant linear function, but also as time dependent for different contract types. With the extract information we price other exotic options.

References

- Alaton, P., Djehiche, B. and Stillberger, D. (2002). On modelling and pricing weather derivatives, *Appl. Math. Finance* **9(1)**: 1–20.
- Barrieu, P. and El Karoui, N. (2002). Optimal design of weather derivatives, *ALGO Research* **5(1)**.
- Benth, F. (2003). On arbitrage-free pricing of weather derivatives based on fractional brownian motion., *Appl. Math. Finance* **10(4)**: 303–324.
- Benth, F. (2004). *Option Theory with Stochastic Analysis: An Introduction to Mathematical Finance.*, Springer Verlag, Berlin.
- Benth, F., Koekebakker, S. and Saltyte Benth, J. (2007). Putting a price on temperature., *Scandinavian Journal of Statistics* .
- Benth, F. and Saltyte Benth, J. (2005). Stochastic modelling of temperature variations with a view towards weather derivatives., *Appl. Math. Finance* **12(1)**: 53–85.
- Brody, D., Syroka, J. and Zervos, M. (2002). Dynamical pricing of weather derivatives, *Quantit. Finance* **3**: 189–198.
- Campbell, S. and Diebold, F. (2005). Weather forecasting for weather derivatives, *American Stat. Assoc.* **100(469)**: 6–16.
- Cao, M. and Wei, J. (2004). Weather derivatives valuation and market price of weather risk, **24(11)**: 1065–1089.
- Davis, M. (2001). Pricing weather derivatives by marginal value, *Quantit. Finance* **1**: 305–308.
- Dornier, F. and Querel, M. (2000). Caution to the wind, *Technical report*, Energy Power Risk Management, Weather risk special report.
- Hamisultane, H. (2006). Extracting information from the market to price the weather derivatives, *Technical report*, Preprint.
- Hull, J. (2006). *Option, Future and other Derivatives*, Prentice Hall International, New Jersey.
- Hung-Hsi, H., Yung-Ming, S. and Pei-Syun, L. (2008). Hdd and cdd option pricing with market price of weather risk for taiwan, *The Journal of Future Markets* **28(8)**: 790–814.
- Ichihara, K. and Kunita, H. (1974). A classification of the second order degenerate elliptic operator and its probabilistic characterization, *Z. Wahrsch. Verw. Gebiete* **30**: 235–254.
- Jewson, S., Brix, A. and Ziehmann, C. (2005). *Weather Derivative valuation: The Meteorological, Statistical, Financial and Mathematical Foundations.*, Cambridge University Press.
- Karatzas, I. and Shreve, S. (2001). *Methods of Mathematical Finance.*, Springer Verlag, New York.
- Malliavin, P. and Thalmaier, A. (2006). *Stochastic Calculus of Variations in Mathematical finance.*, Springer Verlag.
- Mraoua, M. and Bari, D. (2005). Temperature stochastic modelling and weather derivatives pricing: empirical study with moroccan data., *Technical report*, Preprint.
- Odening, M., Muhoff, O. and Xu, W. (2007). Analysis of rainfall derivatives using daily precipitation models: Opportunities and pitfalls., *Technical report*.
- Platen, E. and West, J. (2005). A fair pricing approach to weather derivatives, *Asian-Pacific Financial Markets* **11(1)**: 23–53.
- Richards, T., Manfredo, M. and Sanders, D. (2004). Pricing weather derivatives, *American Journal of Agricultural Economics* **86(4)**: 1005–10017.
- Turvey, C. (1999). The essentials of rainfall derivatives and insurance, *Technical report*, Working Paper WP99/06, Department of Agricultural Economics and Business, University of Guelph, Ontario.

SFB 649 Discussion Paper Series 2009

For a complete list of Discussion Papers published by the SFB 649, please visit <http://sfb649.wiwi.hu-berlin.de>.

- 001 "Implied Market Price of Weather Risk" by Wolfgang Härdle and Brenda López Cabrera, January 2009.
- 002 "On the Systemic Nature of Weather Risk" by Guenther Filler, Martin Odening, Ostap Okhrin and Wei Xu, January 2009.

SFB 649, Spandauer Straße 1, D-10178 Berlin
<http://sfb649.wiwi.hu-berlin.de>

This research was supported by the Deutsche
Forschungsgemeinschaft through the SFB 649 "Economic Risk".

